

Structural and dynamical properties of metastable Al:Si solid solutions calculated by the embedded-atom method

Silvia Rubini

Dipartimento di Fisica "A. Volta," Università di Pavia, via Bassi 6, I-27100 Pavia, Italy

Pietro Ballone

Institut für Festkörperforschung, Forschungszentrum Jülich, D-52425 Jülich, Germany

(Received 31 March 1994; revised manuscript received 20 July 1994)

Metastable fcc $\text{Al}_{1-x}\text{Si}_x$ solid solutions in the low Si concentration range are modeled by the embedded-atom method. The potential parameters for Si are fitted to the experimental lattice constant of the solutions, the cohesive energy, and the elastic properties of the metallic simple-cubic phase of Si determined by *ab initio* computations. The model reproduces and explains the concentration dependence of the vibrational density of states, the decrease of the shear modulus with increasing x , and allows us to simulate the first stages of the alloy decomposition into Al and Si.

Supersaturated solid solutions are perhaps the most common phase for alloys of metallurgical interest, and play a major role among high resistance materials. Recently, Al:Si solid solutions with up to $\sim 30\%$ in Si have been prepared by quenching from the liquid¹ and/or solidification under high pressure^{2,3} (see also Ref. 4 for previous experimental reports). At low pressure and temperature these alloys are metastable and have been characterized by x-ray and neutron diffraction, differential scanning calorimetry, and resistivity measurements.¹ In the concentration range $x \leq 0.10$ the alloy $\text{Al}_{1-x}\text{Si}_x$ is homogeneous and displays clear diffraction peaks corresponding to the Al fcc lattice. Addition of Si destabilizes the Al lattice progressively, as revealed by the softening of the vibrational density of states and of the shear modulus.

Despite these interesting results, we know of no extensive theoretical investigation aimed at clarifying the microscopic properties of Al:Si alloys. In the present study we analyze the structural, elastic, and dynamical properties of Al:Si solutions within the framework of the embedded-atom method⁵ (EAM). The results presented below show that the EAM potential reproduces the experimental dependence of the vibrational density of states (DOS) on the Si concentration. In particular, it displays a clear enhancement in the low frequency DOS that is reflected in the linear decrease with x of the shear modulus C' . Analysis of the eigenfrequencies and eigenvectors shows that the low frequency modes induced by alloying are localized phonons associated with Si enriched regions. Room temperature molecular dynamics (MD) simulations for $\text{Al}_{0.90}\text{Si}_{0.10}$ show that the Si atoms are characterized by large amplitude anharmonic oscillations. With increasing T , we observe the first stages of Si segregation, which occurs by the concerted exchange of one Si atom and several of its neighbors. The interest of the EAM potential we introduce goes beyond the specific system under investigation: as discussed below, the potential for Si can be used, without further fitting, to model a large class of glass forming metallic silicides.

The basis of our model is the experimental evidence that Si is in a metallic state, reverting to semiconductor upon

demixing. We therefore use the EAM to model both Al and Si in the alloy. Within this scheme, the cohesive energy of the system is written:

$$E_c = \frac{1}{2} \sum_{ij} \phi_{ij}(r_{ij}) + \sum_i F_i[\rho_i],$$

where ϕ_{ij} is a short range repulsive potential, assumed to be of the screened Coulomb form:

$$\phi_{ij}(r) = Z_i(r)Z_j(r)/r,$$

with

$$Z_i(r) = Z_i^{(0)}(1 + \beta r^\nu) \exp(-\alpha r).$$

The function F_i describes the energy gain in embedding the atom i in the valence electron density $\rho(\vec{r}_i)$ of all the other atoms:

$$\rho(\vec{r}_i) = \sum_{i \neq j} \rho^{(at)}(|\vec{r}_i - \vec{r}_j|)$$

and $\rho^{(at)}(r)$ is a charge distribution assumed to be the superposition of the (spherically symmetric) atomic charges contributed by the s and p valence electron orbitals of Al or Si:⁶

$$\rho^{(at)}(r) = N_s |\Psi_s(r)|^2 + [N_v - N_s] |\Psi_p(r)|^2. \quad (1)$$

In the expression above, N_v is the valence charge of Al or Si, and N_s is an adjustable parameter. We fit the potential for Al to the experimental lattice constant a_0 , cohesive energy E_0 , bulk modulus B , and elastic constants C_{ij} .⁷ The equation of state in a range of densities around the equilibrium one is approximated by the Rose, Smith, Guinea, and Ferrante (RSGF) expression.⁸ The resulting potential provides phonon dispersion relations and a vibrational DOS (reported below) in good agreement with experiments for low and intermediate frequencies, while it does not describe quantitatively the shape of the peak in the DOS at ~ 9 THz. These same features are observed in the DOS computed from previous EAM potentials for Al.⁷

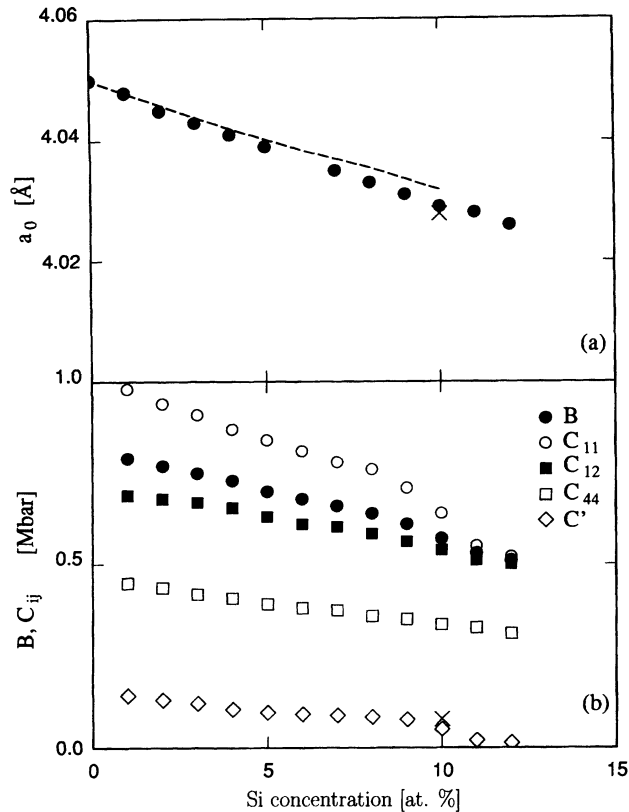


FIG. 1. (a) Computed (dots) and experimental (dash line) lattice constant a_0 of Si:Al alloys as a function of composition. (b) Computed bulk modulus B and elastic constants of Al:Si as a function of composition. The crosses at $x=0.10$ display the a_0 and C' of the annealed samples (see text).

To model Si in a metallic environment, we fit the EAM potential to the cohesive and elastic properties of Si in the metallic simple cubic (sc) phase computed by the pseudopotential density functional–local density approximation method.^{9,10} We have selected this phase because of its simplicity, and because its (metastable) equilibrium volume ($V_0=15.96 \text{ \AA}^3/\text{atom}$) is close to that of Al ($V_0=16.61 \text{ \AA}^3/\text{atom}$). The β -tin phase of Si shares with the sc structure the property of being metallic and having an atomic volume matching that of Al. Moreover, it is energetically slightly more stable and therefore could provide another starting point for the fit of the Si potential. However, it is difficult to reproduce by EAM the precise distances and angles of the *ab initio* Si β tin,¹⁵ and for this reason we have preferred the sc as a basis for our parametrization. To describe the equation of state for volumes different from the equilibrium one we used the Murnaghan equation,¹⁶ which approximates the sc total energy better than the RSGF.

As reported in the literature,¹¹ the fit to the elemental properties is only weakly dependent on the parameter N_s in Eq. (1), while the ratio of the N_s 's for different elements determines their cross interaction. We vary this ratio to fit the experimental lattice constant $a_0(x)$ of the Al:Si solid solutions.¹⁷ The quality of the fit (see Fig. 1) is mainly limited by the fact that each sample with a finite number of atoms (864 in our computation) has slightly different values

TABLE I. Optimal values for the potential of Al and Si.

	Z_0 (e)	α (Å)	β	ν	N_s	R_c (Å)
Al	3	1.315	3.781	0.326	1.90	5.5
Si	3.2	0.551	298.353	-8.906	0.8	4.8

of the lattice parameter; that, moreover, depends (again slightly) on the sample preparation. The enthalpy of mixing turns out to be positive, in agreement with the fact the alloy is metastable ($\Delta H=54 \text{ kJ}$ per Si mole at $x=0.10$, and slowly decreasing with x . This should be compared with the 38 kJ/mole reported in Ref. 2 for the $0 \leq x \leq 0.10$ compositions.) With their ratio chosen in this way, the absolute value of the N_s 's parameters for Al and Si has been determined by the alloying properties of Al with a set of transition and post-transition metals (Ni, Pd, Pt, Au) whose potentials had been prepared and tested independently. Finally, we verified that the Si potential gauged on Al *only* can be combined with those of the enlarged set to describe reliably a series of glass forming metal silicides.¹⁰ The optimal potential parameters for Al and Si are listed in Table I.

We remark that our recipe is slightly different from the one described in the original paper on the EAM modeling of alloys,¹¹ which used the properties of dilute impurities to fit the cross interactions, and focused on the enthalpy of mixing instead of structural properties. We choose to determine N_s from the properties of intermetallic compounds because we expected this to be more reliable for alloys of finite concentration. In fact, by comparing for a few cases the potentials obtained by fitting the properties of impurities and intermetallic compounds we concluded that the two choices produce equivalent potentials. We decided to fit structural data because these are available for a large number of intermetallics at low T . Enthalpy, instead, is usually tabulated only for high T , and this makes less straightforward or less reliable its usage in the fit. Moreover, in our experience lattice constant and excess enthalpy of alloys are, to a large extent, equivalent properties: larger lattice constants usually imply lower mixing enthalpy, and fitting one or the other property provides again equivalent potentials.

Several other potentials have been proposed to model Si within the EAM.¹² Most of these potentials aim to describe the full variety of Si structures by adding either angular forces (see, for instance, Ref. 13), or contributions describing the electron kinetic energy.¹⁴ Our potential has been devised for a more specific task, i.e., to model Si in a metallic environment. It is simple and can easily be combined with EAM potentials for other metals to model a variety of alloys.¹⁰ Deriving our fit from the metallic phase of Si could result in a potential whose global energy surface is very different from the experimental or *ab initio* one. Nevertheless, it turns out that our model has the diamond as metastable structure, with computed cohesive and elastic properties ($a_0=5.637 \text{ \AA}$, $E_0=4.65 \text{ eV/atom}$, $B=1.49 \text{ Mbar}$, $C_{11}=1.65 \text{ Mbar}$, $C_{12}=1.40 \text{ Mbar}$, $C_{44}=0.86 \text{ Mbar}$) not too far from the experimental ones. Only upon heating beyond $\sim 500 \text{ K}$ does the simulated system transform from the diamond to a lower energy structure ($E_0=4.76 \text{ eV/atom}$), which we expect to be the ground state for our potential (a long MD annealing did not find a more stable configuration). Although deformed,

this last structure has—in common with the diamond phase—the properties of being fourfold coordinated with an atomic volume significantly larger than that of Al. Although the description of the pure silicon low energy structure is far from quantitative, it is at least qualitatively correct and we should be able to simulate the first stages of the Al and Si demixing, when the silicon environment is still composed mainly of Al.

Samples of 864 atoms with Si concentration $x \leq 0.15$ have been constructed following two different prescriptions. A few of the samples have been prepared by mimicking the experimental procedure, i.e., by quench from the liquid under high pressure ($P=50$ GPa). This procedure always produced glassy samples, even with the lowest attainable cooling rate ($K=2.5 \times 10^{12}$ K/s, corresponding to 5×10^5 MD steps of 1.571×10^{-15} s). This result is not surprising when one considers the huge difference between simulation and experimental [$K_{\text{exp}}=10^6$ K/s (Ref. 1)] cooling rates. Most of the samples were therefore prepared in the crystal phase by random substitution with Si of the Al atoms in the fcc lattice. The samples prepared by these two methods have similar elastic properties, and we expect that the inability to produce crystal alloys by MD is not a crucial limitation.

We have evaluated the elastic properties of the alloy using static computations. The bulk modulus B and the elastic constants C_{11} , C_{12} , $C' = \frac{1}{2}(C_{11} - C_{12})$ and C_{44} are computed by numerical differentiation with respect to the lattice deformations described in Ref. 18. For each volume and deformation the energy is accurately minimized by relaxing the atomic positions. The results are reported in Fig. 1(b), which shows the progressive softening of the system with increasing Si concentration. Particularly noticeable is the decrease of C' with x that is in agreement with the experimental evidence. The vanishing of C' predicts $x \sim 0.14$ as the limiting composition for the stability of the random alloy. At finite T , however, the first stages of the Si segregation will occur within microscopic times (see the description of our MD simulation below), thus reducing the excess enthalpy and stabilizing the alloy (no longer homogeneous and random) over a wider range of nominal compositions.

The softening of the elastic properties is reflected in the x dependence of the vibrational density of states (DOS), computed by diagonalization of the dynamical matrix at the Γ point of the 864 atom supercell. The results have been convoluted with a Gaussian broadening of 0.4 THz to simulate the experimental resolution of ~ 2 meV,² and are displayed in Fig. 2. Despite the quantitative discrepancies in the high frequency DOS of Al discussed above, the comparison with the experimental results in Refs. 1 and 2 shows that the model is able to describe the changes in the DOS induced by the Si alloying. The low frequency portion of the DOS acquires more weight as x increases, compensated by a decrease of the two Al peaks at 5.8 and 9 THz. The x dependence is more pronounced at low x , and saturates at higher concentration.

Displacement patterns (described by the eigenvectors of the dynamical matrix) show that the low frequency modes induced by the alloying are localized. At low x they involve mainly the Si atoms. At higher x ($x \sim 0.10$) they involve both Si and Al atoms in regions enriched in Si (we observe that Al atoms with at least two Si neighbors participate in the local-

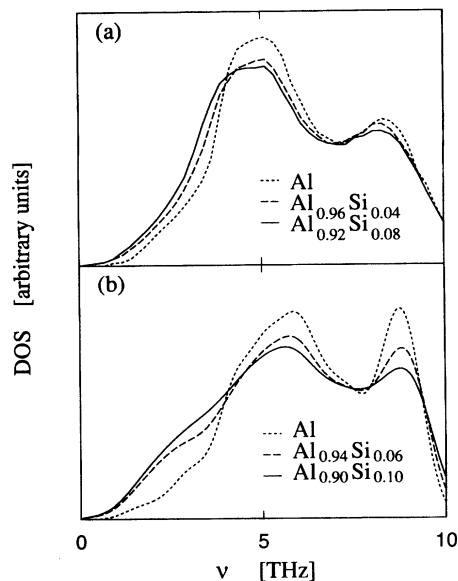


FIG. 2. Vibrational density of states as a function of composition. (a) Experiment; (b) present computation.

ized modes). Modes up to 1.5 THz tend to have a large positive Grüneisen coefficient, signaling the onset of thermal instability in the lattice.

To further explore the anharmonic effects we have performed MD simulations for $\text{Al}_{0.90}\text{Si}_{0.10}$ starting from room temperature.¹⁹ At the lowest T the alloy does not present any important evolution on the time scale of the simulation (~ 11 psec at each temperature). Analysis of trajectories shows that the Si atoms perform low frequency, high elongation oscillations around their equilibrium positions (at $T=300$ K the mean square displacement is 0.265 Å for Si and 0.170 Å for Al). Starting from $T=500$ K we observe the first stages of the Si segregation. To highlight its mechanism we split the simulation into runs of 5000 steps each (corresponding to 7.9 psec), and we compute the displacement of each atom during this time. In most of the runs and for most of the atoms the evolution is qualitatively similar to that observed at lower T , with atomic displacements much shorter than a nearest neighbor distance. Occasionally, however, we observe jumplike events in which one Si atom and several of its neighbors display a displacement comparable to the nearest neighbor separation. The process could be described as a localized melting centered on the Al impurity²⁰ that terminates when the diffusing Si finds another equilibrium position close to another Si atom or cluster.

We have presented a simple interatomic potential of the EAM type that is able to describe a variety of structural, elastic, and dynamical properties of the metastable Al:Si alloys. Microscopic analysis by diagonalization of the dynamical matrix and MD simulation shows that the Si alloying progressively softens the vibrational density of states, first inducing low frequency localized modes and subsequently, at higher T or concentration, locally destabilizing the lattice. The interest in the model is enhanced by the observation that the Si potential can be used to model a large class of glass forming metallic silicides *without further fitting*. Preliminary

computations for $\text{Pd}_{1-x}\text{Si}_x$ and $\text{Au}_{1-x}\text{Si}_x$ ($x \leq 0.20$) show that the model can describe the structure and equilibrium density, the lowering of the melting temperature down to an eutectic point around $x=0.20$, and the elastic properties of these alloys.

Recently, we became aware of an *ab initio* computation for a Si impurity in an Al matrix.²¹ A careful comparison shows that the results of the two computations are in good agreement, and underlines the complementary role of *ab initio* and semiempirical methods: *ab initio* computations are

useful for their intrinsic reliability and because they provide information on the electronic structure otherwise unavailable. Semiempirical methods, however, are required for a wide and inexpensive analysis of the statistical and dynamical properties of large systems.

We are indebted to Stefano de Gironcoli for the *ab initio* computations of the structural and elastic properties of sc Si. We also thank him for useful discussions. We thank R. O. Jones for a careful reading of the manuscript.

-
- ¹J. Chevrier, D. Pavuna, and F. Cyrot-Lackmann, *Phys. Rev. B* **36**, 9115 (1987).
- ²J. Chevrier, J. B. Suck, J. J. Capponi, and M. Perroux, *Phys. Rev. Lett.* **61**, 554 (1988); J. Chevrier *et al.*, *Europhys. Lett.* **8**, 173 (1989); J. Chevrier *et al.*, *Phys. Rev.* **49**, 961 (1994).
- ³V. F. Degtiareva, *et al.*, *Phys. Status Solidi A* **89**, K127 (1985).
- ⁴F. Meunier *et al.*, *Phys. Lett.* **37**, 287 (1968); C. C. Tsuei and W. L. Johnson, *Phys. Rev. B* **9**, 4742 (1974).
- ⁵M. S. Daw and M. I. Baskes, *Phys. Rev. Lett.* **50**, 1285 (1983); M. S. Daw and M. I. Baskes, *Phys. Rev.* **29**, 6443 (1984).
- ⁶E. Clementi and C. Roetti, *At. Data Nucl. Data Tables* **14**, 177 (1974).
- ⁷Our potential for Al is equivalent to those of the following: S. M. Foiles and M. S. Daw, *J. Mater. Res.* **2**, 5 (1987); S. P. Chen, A. F. Voter, and D. J. Srolovitz, *Scr. Metall.* **20**, 1389 (1986).
- ⁸J. H. Rose, J. R. Smith, F. Guinea, and J. Ferrante, *Phys. Rev. B* **29**, 1963 (1984).
- ⁹Stefano de Gironcoli (private communication): $E_0=4.30$ eV, $a_0=2.518$ Å, $B=1.04$ Mbar, $C_{11}=2.23$ Mbar, $C_{12}=0.44$ Mbar, and $C_{44}=0.20$ Mbar. The computed a_0 and E_0 are in good agreement with those reported by M. T. Yin and M. L. Cohen, *Phys. Rev. B* **26**, 5668 (1982).
- ¹⁰S. Rubini and P. Ballone (unpublished).
- ¹¹S. M. Foiles, M. I. Baskes, and M. S. Daw, *Phys. Rev. B* **33**, 7983 (1986).
- ¹²A. E. Carlsson, *Solid State Phys.* **43**, 1 (1990).
- ¹³M. I. Baskes, *Phys. Rev. Lett.* **59**, 2666 (1987).
- ¹⁴A. E. Carlsson, P. A. Fedder, and C. W. Myles, *Phys. Rev. B* **41**, 1247 (1990).
- ¹⁵A β -tin structure for Si is metastable within our EAM potential, with an energy comparable to that of the sc ($E_0=4.19$ eV/atom). It is, however, slightly distorted with respect to its *ab initio* counterpart.
- ¹⁶F. D. Murnaghan, *Proc. Natl. Acad. Sci. U.S.A.* **30**, 5390 (1944).
- ¹⁷B. Predel, in *Phase Equilibria of Binary Alloys*, edited by O. Madelung, Landolt-Börnstein, New Series, Group IV, Vol. 5 (a) (Springer-Verlag, Berlin, 1991), p. 242.
- ¹⁸J. E. Osburn, M. J. Mehl, and B. M. Klein, *Phys. Rev. B* **43**, 1805 (1991).
- ¹⁹The equations of motion have been integrated by the velocity Verlet algorithm with a time step of 1.571×10^{-15} .
- ²⁰E. A. Stern and K. Zhang, *Phys. Rev. Lett.* **60**, 1872 (1988).
- ²¹A. Caro, D. A. Drabold, and O. F. Sankey, *Phys. Rev. B* **49**, 6647 (1994).